EMIC waves growth and guiding in the presence of cold plasma density irregularities

M. de Soria-Santacruz,[1] M. Spasojevic,[2,3] and L. Chen[4]

[1] Intense electromagnetic ion cyclotron (EMIC) waves are observed within plasmaspheric plumes during geomagnetic storms and are believed to be a significant driver of loss of both ring current protons and radiation belt electrons. In this study, we use ray tracing together with path-integrated linear growth calculations to analyze the amplification and propagation of EMIC waves within cold plasma density irregularities characteristic of the plasmaspheric plume. All waves are launched at the equator in the range of $L = 5$ to 7, and wave amplification is analyzed as a function of frequency and initial wave normal angle. These results are compared to a baseline case without irregularities, which show that guiding is possible for irregularity sizes on the order of the EMIC wavelength. Results suggest that typical structures with density levels above and below the average value can result in both areas of increased as well as suppressed wave activity. **Citation:** de Soria-Santacruz, M., M. Spasojevic, and L. Chen (2013), EMIC waves growth and guiding in the presence of cold plasma density irregularities, *Geophys. Res. Lett.*, *40*, doi:10.1002/grl.50484.

1. Introduction

[2] Cyclotron resonant interactions driven by electromagnetic ion cyclotron waves (EMIC) in the Earth's magnetosphere result in pitch angle scattering and subsequent precipitation into the atmosphere of both energetic protons [*Erlandson and Ukhorskiy*, 2001; *Spasojevic et al.*, 2004; *Yahnin and Yahnina*, 2007; *Sakaguchi et al.*, 2008] and relativistic electrons [*Lorentzen et al.*, 2000; *Meredith et al.*, 2003; *Miyoshi et al.*, 2008; *Rodger et al.*, 2008]. EMIC waves propagate below the proton gyrofrequency, and they appear in multiple frequency bands due to the presence of heavy ions, which strongly modify wave propagation characteristics introducing stop bands and polarization reversals. Ray tracing codes, which use the eikonal approximation of geometrical optics to follow the wave group velocity for given magnetic field and plasma density models, have been developed to study the propagation of EMIC waves in the context of in situ observations [*Gomberoff and Neira*, 1983; *Ludlow*, 1989; *Rauch and Roux*, 1982].

[3] EMIC waves are generated by ion cyclotron instability of ring current ions, whose temperature anisotropy provides the free energy required for wave growth. In the presence of sufficiently large ion anisotropy, waves will grow and scatter the particles until the distribution has stabilized. Growth maximizes for magnetic field-aligned propagation near the equatorial plane where the *B*-field curvature is small. Although the group velocity typically stays aligned with the *B*-field direction, wave normal vectors tend to become oblique due to the curvature and gradient of the *B*-field. On the other hand, radial density gradients have the ability to guide the waves and act against the magnetic field effect thus favoring wave growth conditions. In addition, enhanced cold plasma density reduces the proton resonant energy to the energy range of the ring current where higher fluxes are available for resonance. Observations show that wave growth is favored at higher *L*-shell regions where the ratio of plasma to cyclotron frequency is larger [*Anderson et al.*, 1992]. The outer plasmasphere and plasmapause regions contain irregular density structure over an extremely wide range of scale sizes, from global scale plume structures, multi-R_E ripples and depletions, to fine-scale (<1000 km) density irregularities [*LeDocq et al.*, 1994; *Spasojevic et al.*, 2003; *Gallagher et al.*, 2005], and these irregularities are believed to play important role in the generation and propagation of plasma waves [e.g., *Lemaire and Gringauz*, 1998, sec. 2.6].

[4] Ray tracing has been widely used to model the guiding of plasma waves within density ducts [*Inan and Bell*, 1977; *Strangeways*, 1986] and is valid for structure size larger than the wavelength. More recently, *Streltsov et al.* [2006] presented a full-wave analysis showing that transverse scale-size irregularities comparable to or smaller than the wavelength are capable of guiding VLF waves although they are inherently leaky in the case of high-density ducts. The guidance of waves results in enhanced convective growth rates since ducts confine the wave to near parallel wave normal [*Thorne and Horne*, 1997]. *Chen et al.* [2009] showed that EMIC waves can be preferentially excited within irregularity structures embedded in high density plasmaspheric plumes due to the effect of the negative density gradients, which keep the wave normal direction field aligned. The growth at higher *L*-shells in the low-density trough was associated with the higher ω_{pe}/ω_{ce} ratio, which enhances EMIC growth due to the reduced ion resonant energy.

[5] In this paper, we calculate the expected growth and propagation characteristics of EMIC waves in the presence of radial cold plasma irregularities and compare to results of a smooth profile of equal average density within the

[1]Department of Aeronautics and Astronautics, Massachusetts Institute of Technology, Cambridge, Massachusetts, USA.

[2]Department of Electrical Engineering, Stanford University, Stanford, California, USA.

[3]Lockheed Martin Advanced Technology Center, Palo Alto, California, USA.

[4]Department of Atmospheric and Oceanic Sciences, UCLA, Los Angeles, California, USA.

Corresponding author: M. de Soria-Santacruz, Department of Aeronautics and Astronautics, Massachusetts Institute of Technology, 77 Massachusetts Avenue, Room 37-375, Cambridge, MA 02139, USA. (mdesoria@mit.edu)
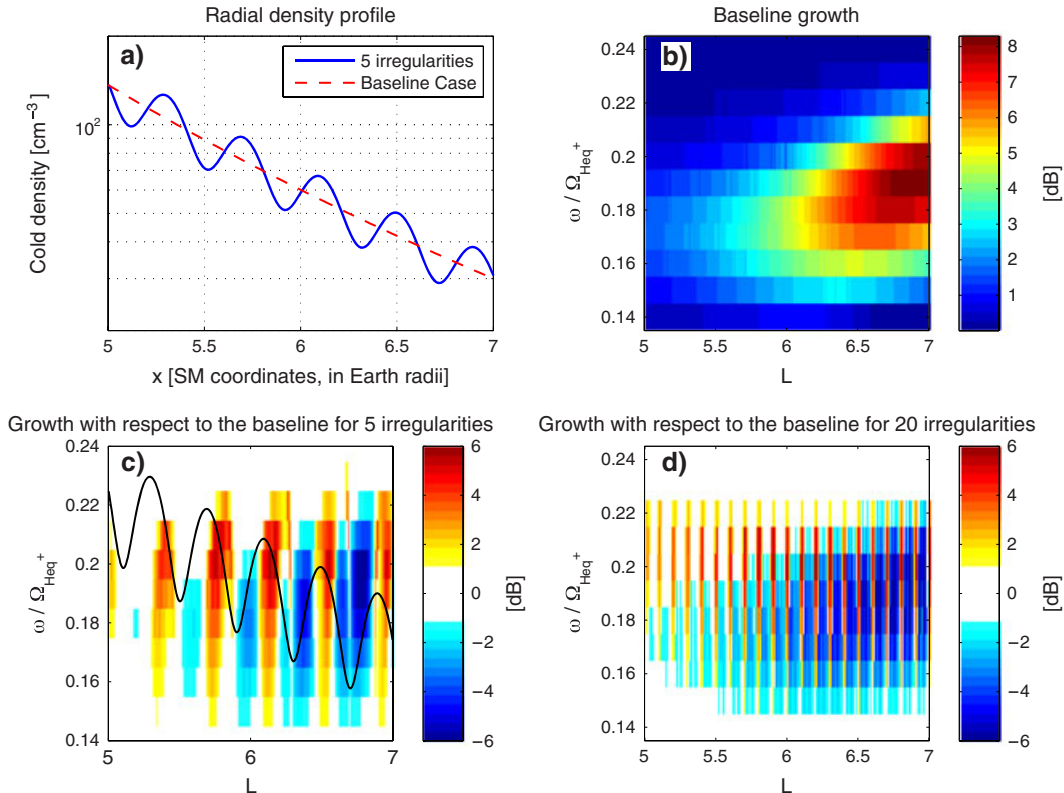
Figure 1. (a) Analytical model of the radial density profile representing the plasmaspheric plume region with five irregularities and 20% variation of the density magnitude (blue). The dashed red line shows the baseline density profile for comparison. (b) Growth as a function of L-shell and normalized frequency for the baseline case without irregularities. (c) Maximum growth with respect to the baseline case as a function of L-shell and non-dimensional frequency for a radial density profile with five irregularities. The solid black line denotes the profile of density variations. (d) Maximum growth with respect to the baseline case as a function of L-shell and non-dimensional frequency for a radial density profile with 20 irregularities.

plasmaspheric plume. The irregularities are generated using an analytical model that resembles the density gradients observed in the plume [*LeDocq et al.*, 1994]. All waves are launched at the equator in the range of $5<L<7$, and wave growth is analyzed as a function of frequency and initial wave normal angle. The results are compared to the baseline case without irregularities, and the effect of the width of the radial density structures is studied and related to wave propagation and guiding.

2. Description of the Model

[6] The simulation uses the International Geomagnetic Reference Field (IGRF) and Tsyganenko [*Tsyganenko*, 1989] magnetic field models with $K_p = 4$ at 12 Magnetic Local Time (MLT). The cold plasma density background within the plasmaspheric plume is taken to fall with increasing L-shell as $L^{-4.5}$ [*Carpenter and Anderson*, 1992] with plume density equal to $N_e = 40$ cm^{-3} at $L = 6.6$ [*Moldwin et al.*, 1995]. The ion composition is taken to be 85% H$^+$, 10% He$^+$, and 5% O$^+$ [*Comfort et al.*, 1988]. We superimpose upon the radial profile cold plasma irregularities with 20% density variations between $L = 5$ to 7, which is a conservative estimate of what is seen in observations [*Goldstein et al.*, 2004; *Spasojevic et al.*, 2003]. Different irregularity widths are analyzed. Thermal electrons, H$^+$, O$^+$, and He$^+$ are assumed to be Maxwellian with temperatures of 10 eV for electrons and 1 eV for ions. Ring current protons are

considered bi-Maxwellian with $T_\parallel = 7.75$ keV and $T_\perp = 11$ keV, which corresponds to a temperature anisotropy of 0.42 and is consistent with observations at geosynchronous orbit [*Spasojevic et al.*, 2005]. The radial cold plasma profile with five irregularities is presented in Figure 1a.

[7] All rays are initiated at the equator between $L = 5$ to 7, and their behavior as a function of the initial wave normal angle and frequency is analyzed. The Stanford VLF 3-D ray tracer [*Golden et al.*, 2010] for the two dimensional case is used together with path-integrated linear growth calculations. Ray tracing uses the geometric optics approximation to determine the trajectory of the ray path. This approximation assumes that the properties of the medium vary slowly within one wavelength and that the plasma is cold, i.e., the thermal velocity of the particles is much smaller than the wave phase velocity [*Haselgrove*, 1955]. Ray tracing using the cold plasma dispersion relation provides wave normal vectors and plasma properties along the ray path, which are inputs to the local convective growth rate calculation. The simulation takes into account the hot and cold plasma populations described above, and Landau ($m = 0$) and the first three cyclotron resonances ($m = \pm 1, \pm 2, \pm 3$) are considered in the integration of the convective growth rate [*Chen et al.*, 2010, equation (2)]. The waves are propagated from the equator for a 100 s interval, and the path-integrated gain is finally calculated by integrating the linear growth rate along the ray path.
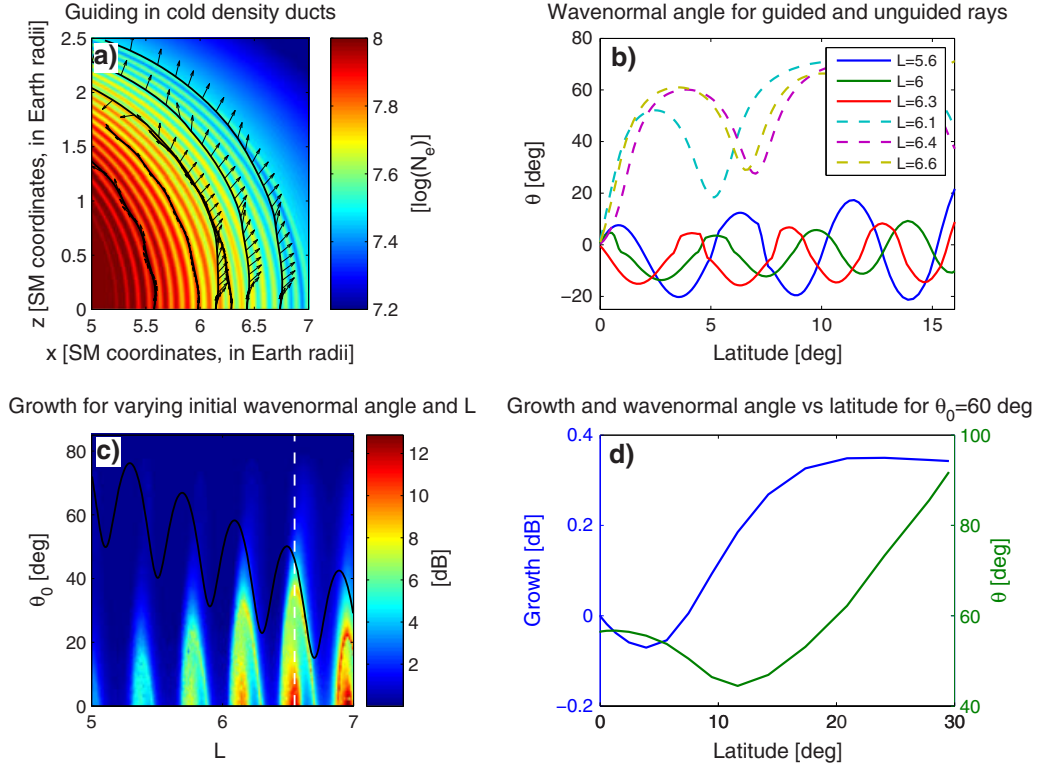
Figure 2. (a) Ray paths and wave normal angles of different rays launched from enhancement and depletion ducts in the 20-irregularity density profile with $\omega/\Omega_{H^+} = 0.2$. (b) Evolution of the wave normal angle as a function of latitude for the rays in (Figure 2a), launched from enhancement (solid lines) and depletion (dashed lines) ducts at different L-shells. (c) Maximum growth as a function of L-shell and initial wave normal angle for a radial density profile with five irregularities and $\omega/\Omega_{H^+} = 0.2$. The solid black line denotes the profile of density variations. (d) Growth and wave normal angle as a function of latitude for the ray in Figure 2c that corresponds to $\theta_0 = 60°$ and $L = 6.55$.

3. Results

[8] Figure 1b presents the maximum path-integrated growth for the baseline plasmaspheric plume without density irregularities versus ω/Ω_{H^+} and L, where Ω_{H^+} is the proton cyclotron frequency at the equator. Growth is only observed in the helium band, between the oxygen crossover and the helium cyclotron frequency, which agrees with observational evidence [*Meredith et al.*, 2003; *Miyoshi et al.*, 2008]. The presence of heavy ions such as He$^+$ lowers the phase speed of the L-mode below the He$^+$ gyrofrequency, which leads to lower ring current proton resonant energies and enhances EMIC growth [*Gomberoff and Neira*, 1983; *Kozyra et al.*, 1984; *Thorne et al.*, 2006]. The growth increases with increasing L-shell due to the effect of ω_{pe}/ω_{ce}, where ω_{pe} and ω_{ce} are the electron plasma and cyclotron frequency, respectively. The ratio ω_{pe}/ω_{ce} increases with increasing L value after $L = 6$, which lowers the proton resonant energy, thus more particles in the distribution can cyclotron resonate and amplify the wave.

[9] Figure 1c presents the maximum path-integrated growth corresponding to the density profile in Figure 1a, where we have subtracted the growth from the baseline case (Figure 1b). All waves are launched parallel to the Earth's magnetic field. The wavelength at the equator ranges between 500–800 km, and the irregularity size is about 2500 km, much larger than the EMIC wavelengths. Growth in the presence of irregularities is up to 6 dB larger than

the baseline, and it is localized in the enhancement density ducts on the negative density gradient side. This gradient is responsible for guiding of the waves along the enhancement ducts, which increases the efficiency of the cyclotron resonant interaction with ring current protons and maximizes growth. On the other hand, depletion ducts tend to suppress the wave growth that was present in the high ω_{pe}/ω_{ce} region of the baseline case. This fact suggests that typical plasmaspheric plume irregularities with cold density levels above and below the average value can generate both areas of increased as well as suppressed wave activity. In addition, we observe that within the negative density gradient of an irregularity, the growth region moves to lower L-shell values for decreasing wave frequency, which results in a shift of each of the five growth patterns with increasing L-shell and wave frequency. This fact is due to the cyclotron resonant condition and the effect of ω_{pe}/ω_{ce}. Within the negative density gradient, the gradient in density is much stronger than the radial variation of the Earth's magnetic field, thus ω_{pe}/ω_{ce} increases when moving to lower L-shells within these regions. Since the temperature of the ring current protons is fixed, lower L-shells translate to a decrease of the resonant frequency for cyclotron interaction, i.e., a shift of the growth patterns with increasing L-shell and wave frequency. A different effect is the observed slip in phase of the peaks in wave growth; this effect is an artifact generated by the process of subtraction of the baseline, which has its own spatial and frequency dependence. The peak abso-

lute growth, however, is always in phase with the negative plasma density slope over all irregularity cycles, which is consistent with *Chen et al.* [2009].

[10] Similarly, Figure 1d presents the maximum path-integrated growth of EMIC waves launched parallel to the Earth's magnetic field in a cold density profile with 20 radial irregularities and the same variation in density magnitude. In this case, the irregularity size is 600 km, which is around the equatorial wavelength of the EMIC waves. Despite the stronger radial density gradients compared to the five-irregularity case, the maximum growth remains 6 dB larger than the baseline, localized again around the negative density gradient. We observe that irregularity sizes of the order of the wavelength are capable of guiding the waves. It must be noted that while our model correctly computes the group velocity and path-integrated gain, it cannot reproduce the loss of wave power due to mode conversion or leakage from the narrow density ducts [*Streltsov et al.*, 2006], which are out of the scope of this study.

[11] Figures 1c and 1d show that EMIC waves only grow in enhancement ducts, not in depletion ducts in contrast to whistler mode waves [e.g., *Bell et al.*, 2009]. This fact is related to wave guiding, which is presented in Figure 2. Figure 2a shows the path of several rays from the 20-irregularity case with a frequency equal to $\omega/\Omega_{H^+} = 0.2$. The arrows along the rays represent the wave normal vector, and the background color indicates the logarithm of the cold plasma density. Figure 2b presents the wave normal angle θ of the rays versus latitude. We observe that the rays launched from density enhancement ducts remain guided while the wave normal vector rapidly becomes oblique when launched from density depletion regions due to the curvature and gradient of the B-field. The dispersion surface of EMIC waves has an asymptote for wave normal vectors close to perpendicular to the external magnetic direction, thus the group velocity is mostly aligned with the Earth's magnetic field. The guiding behavior is due to the shape of this surface. Guiding in a depletion duct would require a convex dispersion surface, which will cause the ray to rotate in the opposite direction of the wave normal vector, thus away from regions of higher refractive index. However, the dispersion of EMIC waves is mostly concave or flat at large wave normal angles. This surface is capable of guiding the waves in enhancement ducts since the ray rotates in the same direction as the wave normal vector in the direction of increasing refractive index. Since guided rays have larger perpendicular wave fields, which increase the efficiency of the cyclotron resonant interaction with ring current protons, enhanced wave growth is observed in these regions. Not only are depletion ducts not capable of guiding the waves, but the decreased cold plasma density tends to reduce growth below the baseline case level.

[12] The only possibility to simulate guiding (and growth) in depletion ducts would be to launch the rays at an oblique wave normal angle that falls in the slightly convex portion of the dispersion surface. The behavior as a function of initial wave normal angle θ_0 is presented in Figure 2c, which displays the maximum path-integrated growth for varying angle and L-shell for the five-irregularity case and $\omega/\Omega_{H^+} = 0.2$. All the rays have been launched with wave normal vectors pointing toward larger L-shells. The growth is stronger for field-aligned waves because the perpendicular wave fields are larger, which increase the efficiency of the cyclotron res-

onant interaction. We do not observe growth in depletion ducts at any θ_0, which suggests that, independent of their propagation angles, EMIC waves would only be observed in enhancement ducts. As we increase the initial wave normal angle, the growth drops as Landau interaction damps the oblique waves, and the growth patterns concentrate around smaller regions of the negative density gradient. However, despite Landau damping, we do observe some growth for very oblique wave normal angles, which is due to the guiding effect caused by the Earth's magnetic field and the radial density gradient. Figure 2d presents the growth and wave normal angle along the propagation path of a ray with $\theta_0 = 60°$ and $L = 6.55$ in the middle of an enhancement duct. At the beginning of the path, the wave normal angle is very large, which causes wave damping due to Landau interaction. Once the ray reaches a latitude of $\lambda = 5°$, the wave normal vector tends to align with the Earth's magnetic field, slight wave growth is observed. After $\lambda = 20°$, the wave normal angle strongly increases again to values larger than $\theta_0 = 60°$ and wave growth ceases.

4. Discussion and Summary

[13] Using an analytical model, we have reproduced the radial cold plasma density irregularities typical of the storm-time plasmaspheric plume. We performed ray tracing and path integrated linear growth calculations to compute the growth of EMIC waves in the presence of these radial irregularities. Growth is only observed in the helium band, between the oxygen crossover and the helium cyclotron frequency. The presence of heavy ions such as He^+ lowers the phase speed of the L-mode below the He^+ gyrofrequency, which leads to lower ring current proton resonant energies and enhances EMIC growth. The growth increases at large L-shell values due to the increase of ω_{pe}/ω_{ce}, which is consistent with previous models [*Chen et al.*, 2009].

[14] We find that wave guiding is possible for irregularity sizes of the order of the EMIC wavelength and that guiding enhances wave growth. We noted that the study does not consider mode conversion or leakage from the density ducts, which could reduce the wave intensity for duct sizes comparable to the wavelength. However, leakage has been found to be small for smooth-walled density channels [*Streltsov et al.*, 2006] like the ones reproduced in this paper, and mode conversion unlikely occurs for the analyzed range of frequencies, which are always above the oxygen crossover frequency. Guided rays maximize growth because the perpendicular fields are larger for field-aligned waves, which increase the efficiency of the cyclotron resonant interaction with ring current protons. EMIC guiding and growth localize in density enhancement ducts on the negative density gradient side. Depletion ducts tend to suppress wave growth compared to the case with no irregularities. We do not observe growth in depletion ducts for any initial wave normal angle. Depletion ducts are not capable of guiding the waves, and the decreased cold plasma density contributes to a reduction of EMIC wave growth below the baseline case level. This fact suggests that typical plasmaspheric plume irregularities with cold density levels above and below the average value can result in both areas of increased as well as suppressed wave activity.

[15] We have showed the effect of the wave normal angle in growth and propagation. Landau interaction damps

the largely oblique waves. However, the Earth's magnetic field and the cold density profile of the enhancement ducts tend to align the wave normal vector with the magnetic direction, which generates a small cyclotron growth for the oblique waves.

[17] The Editor thanks two anonymous reviewers for their assistance in evaluating this paper.

References

Anderson, B. J., R. E. Erlandson, and L. J. Zanetti (1992), A statistical study of, Pc 1-2 magnetic pulsations in the equatorial magnetosphere, 2. Wave properties, *J. Geophys. Res.*, *97*(A3), 3089–3101, doi:10.1029/91JA02697.

Bell, T., U. Inan, N. Haque, and J. Pickett (2009), Source regions of banded chorus, *Geophys. Res. Lett.*, *36*, L11101, doi:10.1029/2009GL037629.

Carpenter, D., and R. Anderson (1992), An ISEE/whistler model of equatorial electron density in the magnetosphere, *J. Geophys. Res.*, *97*(A2), 1097–1108, doi:10.1029/91JA01548.

Chen, L., R. M. Thorne, and R. B. Horne (2009), Simulation of EMIC wave excitation in a model magnetosphere including structured high-density plumes, *J. Geophys. Res.*, *114*, A07221, doi:10.1029/2009JA014204.

Chen, L., R. M. Thorne, V. K. Jordanova, C. P. Wang, M. Gkioulidou, L. R. Lyons, and R. B. Horne (2010), Global simulation of EMIC wave excitation during the 21 April 2001 storm from coupled ECM-RAM-HOTRAY modeling, *J. Geophys. Res.*, *115*, A07209, doi:10.1029/2009JA015075.

Comfort, R. H., I. T. Newberry, and C. R. Chappell (1988), Preliminary statistical survey of plasmaspheric ion properties from observations by DE-1/RIMS, in *Modeling Magnetospheric Plasma*, edited by T. E. Moore, and J. H. Waite Jr., pp. 288–114, AGU, Washington, D. C.

Erlandson, R. E., and A. J. Ukhorskiy (2001), Observations of electromagnetic ion cyclotron waves during geomagnetic storms: Wave occurrence and pitch angle scattering, *J. Geophys. Res.*, *106* (A3), 3883–3895, doi:10.1029/2000JA000083.

Gallagher, D., M. Adrian, and M. Liemohn (2005), Origin and evolution of deep plasmaspheric notches, *J. Geophys. Res.*, *110*, A09, doi:10.1029/2004JA010906.

Golden, D. I., M. Spasojevic, F. R. Foust, N. G. Lehtinen, N. P. Meredith, and U. S. Inan (2010), Role of the plasmapause in dictating the ground accessibility of ELF/VLF chorus, *115*, A11211, doi:10.1029/2010JA015955.

Goldstein, J., B. Sandel, M. Thomsen, M. Spasojevic, and P. Reiff (2004), Simultaneous remote sensing and in situ observations of plasmaspheric drainage plumes, *J. Geophys. Res.*, *109*, A03202, doi:10.1029/2003JA010281.

Gomberoff, L., and R. Neira (1983), Convective, growth rate of ion cyclotron waves in a $H^+ - He^+$ and $H^+ - He^+ - O^+$ plasma, *J. Geophys. Res.*, *88*(A3), 2170–2174, doi:10.1029/JA088iA03p02170.

Haselgrove, J. (1955), Ray theory and a new method for ray tracing, in *Physics of the Ionosphere, Report of the Conference held at the Cavendish Laboratory, Cambridge*, September, 1954, 355 p., The Physical Society, London.

Inan, U. S., and T. F. Bell (1977), The plasmapause as a VLF wave guide, *J. Geophys. Res.*, *82*(19), 2819, doi:10.1029/JA082i019p02819.

Kozyra, J., T. Cravens, A. Nagy, E. Fontheim, and R. Ong (1984), Effects of energetic heavy ions on electromagnetic ion cyclotron wave generation in the plasmapause region, *J. Geophys. Res.*, *89*(A4), 2217–2233, doi:10.1029/JA089iA04p02217.

LeDocq, M., D. Gurnett, and R. Anderson (1994), Electron number density fluctuations near the plasmapause observed by the CRRES spacecraft, *J. Geophys. Res.*, *99*, 23–23, doi:10.1029/94JA02294.

Lemaire, J., and K. Gringauz (1998), *The Earth's Plasmasphere*, Cambridge University Press, New York, NY.

Lorentzen, K. R., M. P. McCarthy, G. K. Parks, J. E. Foat, R. P. Lin, R. M. Millan, D. M. Smith, and J. P. Treilhou (2000), Precipitation of relativistic electrons by interaction with electromagnetic ion cyclotron waves, *J. Geophys. Res.-Space Physics*, *105*(A3), 5381–5389, doi:10.1029/1999JA000283.

Ludlow, G. R. (1989), Growth of obliquely propagating ion cyclotron waves in the magnetosphere, *J. Geophys. Res.*, *94*(A11), 15,385–15,391, doi:10.1029/JA094iA11p15385.

Meredith, N. P., R. M. Thorne, R. B. Horne, D. Summers, B. J. Fraser, and R. R. Anderson (2003), Statistical analysis of relativistic electron energies for cyclotron resonance with EMIC waves observed on CRRES, *J. Geophys. Res.*, *108*, doi:10.1029/2002JA009700.

Miyoshi, Y., K. Sakaguchi, K. Shiokawa, D. Evans, J. Albert, M. Connors, and V. Jordanova (2008), Precipitation of radiation belt electrons by EMIC waves, observed from ground and space, *Geophys. Res. Lett.*, *35*, doi:10.1029/2008GL035727.

Moldwin, M. B., M. F. Thomsen, S. J. Bame, D. McComas, and G. D. Reeves (1995), The fine-scale structure of the outer plasmasphere, *J. Geophys. Res.*, *100*(A5), 8021–8029, doi:10.1029/94JA03342.

Rauch, J. L., and A. Roux (1982), Ray tracing of ULF waves in a multicomponent magnetospheric plasma: Consequences for the generation mechanism of ion cyclotron waves, *J. Geophys. Res.*, *87*(A10), 8191–8198, doi:10.1029/JA087iA10p08191.

Rodger, C. J., T. Raita, M. A. Clilverd, A. Seppälä, S. Dietrich, N. R. Thomson, and T. Ulich (2008), Observations of relativistic electron precipitation from the radiation belts driven by EMIC waves, *Geophys. Res. Lett.*, *35*, doi:10.1029/2008GL034804.

Sakaguchi, K., K. Shiokawa, Y. Miyoshi, Y. Otsuka, T. Ogawa, K. Asamura, and M. Connors (2008), Simultaneous appearance of isolated auroral arcs and Pc 1 geomagnetic pulsations at subauroral latitudes, *J. Geophys. Res.*, *113*, A05,201, doi:10.1029/2007JA012888.

Spasojevic, M., J. Goldstein, D. Carpenter, U. Inan, B. Sandel, M. Moldwin, and B. Reinisch (2003), Global response of the plasmasphere to a geomagnetic disturbance, *J. Geophys. Res.*, *108*(A9), 1340, doi:10.1029/2003JA009987.

Spasojevic, M., H. Frey, M. Thomsen, S. Fuselier, S. Gary, B. Sandel, and U. Inan (2004), The link between a detached subauroral proton arc and a plasmaspheric plume, *Geophys. Res. Lett.*, *31*, L04803, doi:10.1029/2003GL018389.

Spasojevic, M., M. F. Thomsen, P. J. Chi, and B. R. Sandel (2005), Afternoon subauroral proton precipitation resulting from ring current – plasmasphere interaction, in *Inner Magnetosphere Interactions: New Perspectives From Imaging, Geophys. Monogr. Ser.*, vol. 159, edited by J. Burch, M. Schulz, and H. Spence, pp. 85–99, AGU, Washington, D. C.

Strangeways, H. J. (1986), Whistler leakage from narrow ducts, *J. Atmos. Sol. Terr. Phys.*, *48*(5), 455–462, doi:10.1016/0021-9169(86)90122-4.

Streltsov, A. V., M. Lampe, W. Manheimer, G. Ganguli, and G. Joyce (2006), Whistler propagation in inhomogeneous plasma, *J. Geophys. Res.*, *111*, A03216, doi:10.1029/2005JA011357.

Thorne, R., and R. Horne (1997), Modulation of electromagnetic ion cyclotron instability due to interaction with ring current O^+ during magnetic storms, *J. Geophys. Res.*, *102*(A7), 14,155–14,163, doi:10.1029/96JA04019.

Thorne, R., R. Horne, V. Jordanova, J. Bortnik, and S. Glauert (2006), Interaction of EMIC waves with thermal plasma and radiation belt particles, *Geophys. Monogr. Ser.*, *169*, 213, doi:10.1029/169GM14.

Tsyganenko, N. (1989), A magnetospheric magnetic field model with a warped tail current sheet, *Planet Space Sci.*, *37* (1), 5–20, doi:10.1016/0032-0633(89)90066-4.

Yahnin, A. G., and T. A. Yahnina (2007), Energetic proton precipitation related to ion-cyclotron waves, *J. Atmos. Sol. Terr. Phys.*, *69*, 1690–1706, doi:10.1016/j.jastp.2007.02.010.